Appendix E

A Selective ^{15}N-to-^{1}H Polarization Transfer Sequence for More Sensitive Detection of ^{15}N-Choline

Reproduced from *Journal of Magnetic Resonance* **2010**, *205*, 125-129

Journal of Magnetic Resonance 205 (2010) 125–129

Contents lists available at ScienceDirect

Journal of Magnetic Resonance

journal homepage: www.elsevier.com/locate/jmr

A selective ^{15}N-to-^{1}H polarization transfer sequence for more sensitive detection of ^{15}N-choline

Jessica A. Pfeilsticker, Jason E. Ollerenshaw, Valerie A. Norton, Daniel P. Weitekamp *

A.A. Noyes Laboratory of Chemical Physics, California Institute of Technology, Pasadena, CA 91125, USA

ARTICLE INFO

Article history:
Received 28 July 2009
Revised 17 March 2010
Available online 27 April 2010

Keywords:
INEPT
PASADENA
^{15}N-choline
Hyperpolarization
Selective coherence transfer
REBURP

ABSTRACT

The sensitivity and information content of heteronuclear nuclear magnetic resonance is frequently optimized by transferring spin order of spectroscopic interest to the isotope of highest detection sensitivity prior to observation. This strategy is extended to ^{15}N-choline using the scalar couplings to transfer polarization from ^{15}N to choline's nine methyl ^{1}H spins in high field. A theoretical analysis of a sequence using nonselective pulses shows that the optimal efficiency of this transfer is decreased by 62% as the result of competing ^{15}N–^{1}H couplings involving choline's four methylene protons. We have therefore incorporated a frequency-selective pulse to support evolution of only the ^{15}N–methyl ^{1}H coupling during the transfer period. This sequence provides a 52% sensitivity enhancement over the nonselective version in *in vitro* experiments on a sample of thermally polarized ^{15}N-choline in D_2O. Further, the ^{15}N T_1 of choline in D_2O was measured to be 217 ± 38 s, the ^{15}N–methyl ^{1}H coupling constant was found to be 0.817 ± 0.001 Hz, and the larger of choline's two ^{15}N–methylene ^{1}H coupling constants was found to be 3.64 ± 0.01 Hz. Possible improvements and applications to *in vivo* experiments using long-lived hyperpolarized heteronuclear spin order are discussed.

1. Introduction

It is now possible to routinely generate samples of certain small biomolecules with nuclear polarizations on the order of 10% using parahydrogen and synthesis allow dramatically enhanced nuclear alignment (PASADENA) [1] or dynamic nuclear polarization (DNP) [2,3]. These technologies show promise for clinical applications based on the *in vivo* characterization of metabolic processes on the seconds timescale. Experiments of this nature rely on storage of the polarization on heteronuclei with long population relaxation times, such as carbonyl ^{13}C or quaternary ^{15}N nuclei, in order to minimize relaxation losses during sample delivery and to provide time for transport, binding, and metabolism. However, the sensitivity enhancement afforded by this strategy is partly lost if the final signal is also detected on a low-γ heteronucleus. Chekmenev et al. [4] have proposed that optimal sensitivity can be obtained by storing polarization on a slowly-relaxing heteronuclear spin and then using an INEPT [5] sequence to coherently transfer magnetization to nearby ^{1}H nuclei for detection, and have demonstrated the method with two hyperpolarized reagents, 1-^{13}C-succinate-d_2 and 2,2,3,3-tetrafluoropropyl 1-^{13}C-propionate-d_3 (TFPP). Those experiments were designed numerically assuming that the relevant ^{1}H and ^{13}C sites were 3-spin ABX systems. A similar strategy has been applied to ^{15}N-choline, where the hyperpolarized ^{15}N polarization was transferred by nonselective INEPT resulting in detectable signal on some of the proton sites [6].

Here we demonstrate a selective version of this polarization transfer strategy with ^{15}N-choline, an $A_9BB'CC'X$ system of 14 spin 1/2 nuclei [7]. Choline is a useful biomarker, showing significantly altered uptake and metabolism in diseased brain tissue [8] and in malignant tumor cells in the breast and prostate [9,10], though toxicity may limit the dose in some applications. Hyperpolarization of ^{15}N-choline to (4.6 ± 1)% has been reported after 2 h of DNP at 1.4 K [3,6]. The ^{15}N longitudinal relaxation time of T_1 = 120 s in blood [3] is promising for metabolic studies.

We have investigated two INEPT-based pulse sequences for ^{15}N-to-^{1}H polarization transfer in ^{15}N-choline. The first is a nonselective refocused INEPT sequence similar to that used in recent hyperpolarized experiments [4,6]. While this sequence is effective, a product operator analysis shows that significantly greater sensitivity can be obtained by using a selective sequence, as demonstrated by targeting choline's nine degenerate methyl ^{1}H spins. We therefore also present a selective refocused INEPT transfer that uses a REBURP pulse to support coherence transfer from ^{15}N to choline's methyl ^{1}H spins while suppressing competing transfer pathways to methylene ^{1}H nuclei. These pulse sequences are experimentally demonstrated *in vitro* using a thermally polarized sample of ^{15}N-choline in aqueous solution.

* Corresponding author. Fax: +1 626 395 6948.
E-mail address: weitekamp@caltech.edu (D.P. Weitekamp).

1090-7807/$ - see front matter © 2010 Elsevier Inc. All rights reserved.
doi:10.1016/j.jmr.2010.04.010

glycoprotein gp41. The performance of that assay is compared against the gold standard chimeric protein antigen using sera collected from a cohort of HIV-1-positive human subjects, plus controls. We also report on the thermal stability of the capture agent cocktail, with an eye towards point-of-care HIV diagnostics assays that are needed in environments where refrigeration chains may not exist.

Materials and Methods

For detailed protocols see **Materials and Methods S1**.

Ethics Statement

All study documents and procedures regarding the patient serum assays were approved by the UCLA and Caltech Institutional Review Boards. All subjects provided written informed consent prior to initiation of study procedures.

Results and Discussion

The development of a PCC Agent against a protein target utilizes the target itself to promote the 1,3-dipolar cycloaddition between an acetylene and an azide group to form a triazole linkage (the *in situ* 'click' reaction) [12]. The protein effectively plays the role of an extremely selective, but much less efficient, variant of the Cu(I) catalyst that is commonly used for such couplings [13,14]. For the present work, the two reacting species are peptides – one peptide (the anchor) is a chemically modified variant of a conserved, immunogenic epitope on the HIV-1 gp41 protein, and the second peptide is selected via an *in situ* click screen from a large (10^6 element) one-bead-one-compound (OBOC) [15] peptide library. The protein targets are human monoclonal antibodies raised against variants of the gp41 epitope represented by the anchor peptide.

The PCC Agents developed here were designed to capture antibodies that are selective for residues 600–612 (IWCGSGK-LICTTA) of gp41. Previous studies have shown that a large fraction of HIV-1-positive patients develop antibodies against this epitope [16,17]. Our strategy for sampling the polyclonal diversity of such antibodies was to develop PCC Agents that exhibited both differential, as well as similar avidities for human monoclonal antibodies (mAbs) raised against different parts of this epitope. A key decision in this regard involves the selection of the anchor peptides from which the PCC Agents are developed. For this task, we modified the polypeptide fragment corresponding to residues 600–612 of gp41 with artificial amino acids at multiple locations, and tested the ability of these modified peptides to detect two different monoclonal anti-gp41 antibodies 3D6 and 4B3 (Polymun, Klosterneuburg, Austria). The 3D6 mAb was raised against the epitope SGKLIC, whereas the 4B3 mAb was raised against SGKLICTTA. One anchor peptide, A21, was synthesized by adding a propargyl glycine (Pra) residue at the C-terminus of the residues 600–612 of gp41. This anchor peptide was also N-terminally tagged with a polyethylene glycol (PEG) oligomer bridge and a biotin label. For a second anchor peptide (A22), Leu-607 was substituted with Pra. A22 also included an N-terminal PEG-biotin label. A21 equally detected 3D6 and 4B3 with an estimated dissociation constant (K_d) of 1–50 nM, while A22 differentially detected 3D6 (K_d>10 μM) and 4B3 (K_d = 1–50 nM) (**Figure S1** in Supporting Information). A21 and A22 were then separately developed into PCC agents against 3D6 and 4B3, respectively.

The *in situ* click screens are illustrated in **Figure 1**. The target IgG is incubated with an excess of the selected anchor peptide and a large OBOC library at 4°C overnight (see **Materials and Methods S1**). The OBOC library is synthesized on TentaGel resin (Rapp Polymere, Tuebingen, Germany), and is a comprehensive library of 5-mers with a 6th amino acid at the N-terminus presenting an azide functionality. To help ensure chemical and biochemical stability, the OBOC library is comprised of non-natural (D) stereoisomers of the 20 natural amino acids, excluding cysteine and methionine. The *in situ* screen is designed to identify a secondary (2°) peptide that, when coupled to the anchor, forms a biligand with increased selectivity and/or affinity for the target IgG. The screen proceeds stepwise. In the first step (not shown in **Figure 1**) the OBOC library is cleared of beads that exhibit non-specific binding to alkaline phosphatase-conjugated streptavidin (SA-AP), which is used as a detection reagent in a later step. Step 2 is a target screen, and so is designed to detect the presence of the bound IgG target to specific beads, and defines possible hits. The step 3 screen is designed to remove those beads from the pool of potential hits that also exhibit binding to off-target serum proteins. Step 4 is called a product screen, and is unique to sequential *in situ* click screens [11]. This screen is designed to detect for the presence of *in situ* clicked reaction products, which are those hit beads containing the triazole-linked anchor peptide. Typically, Step 2 yields a few hundred hits (~0.05% of the OBOC library). Step 3 reduces that pool by a factor of 2 or 3 to about 100 hits, and Step 4 further reduces the number of hits to around 10. This is a manageable number, meaning that each hit can be separately synthesized as a biligand using Cu(I) catalyzed click chemistry to couple the anchor and 2° peptides. The performance of these biligands is then characterized using immunoprecipitation (pull-down) assays detected by Western blotting from spiked serum samples for specificity (data not shown), and sandwich ELISAs and surface plasmon resonance (SPR) assays for affinity estimations (**Figure S2, Figure S3**). A complete list of the hits for the A21/3D6 and A22/4B3 screens is given in **Table S1**. This approach yielded two equivalently performing biligands against 3D6, and one biligand against 4B3 (**Figures S2, Figure S3**). These three PCC agents (**Figure 2**) were combined, in equal parts, to form a capture agent cocktail. The cocktail slightly outperformed both the standard commercial chimeric antigen and A21, when tested against healthy human serum spiked with both 3D6 and 4B3 (**Figure S4**). A21 is the equivalent of the original antigenic epitope of gp41.

The PCC Agent cocktail and the standard antigen were co-evaluated against a panel of clinical samples using sandwich ELISAs. Serum samples were collected from nine HIV-1-positive patients in Southern California. The standard antigen is a recombinant chimeric protein containing a fragment of HIV-1 gp41 (residues 546–692), the "O" group HIV-1 gp41 immunodominant region (residues 580–623), and a fragment of HIV-2 gp36 (residues 591–617). A good performance of this chimeric antigen has been reported elsewhere [18]. For the comparison assays, streptavidin-coated 96-well plates were saturated with the PCC Agent cocktail or chemically biotinylated chimera in triplicates. Serum samples were diluted to 1% v/v in Tris-buffered saline (TBS) supplemented with 0.1% w/v bovine serum albumin (BSA), and incubated in the wells for 1 hr at room temperature. Unbound proteins were washed off and captured IgG was detected with a peroxidase-conjugated mouse monoclonal anti-human IgG-Fc antibody. The comparison assay results for the patient serum samples along with a healthy control are shown in **Figure 3A**. The signal-to-noise (S/N) ratio in these assays is defined as the measured ELISA signal for a given patient sample, divided by that for the healthy control. The PCC Agent cocktail performed at least as well, and typically much better, than the standard chimeric

A proportionality constant A_{non} and a DC offset constant C have again been included. Maximizing this function numerically for the best known values of the three coupling constants for choline, J_m = 0.82 Hz, J_a = −0.57 Hz, J_b = 3.64 Hz, gives an optimal transfer delay τ_1 = 0.233 s, which yields a signal of $S_{non} = 0.721A_{non} + C$.

Comparing the maximum values of S_{sel} and S_{non}, it is apparent that the ^{15}N–methylene ^{1}H couplings have the effect of reducing the observable ^{1}H signal by 62% in the idealized case of an experiment for which $A_{sel} = A_{non}$ and $C = 0$. It would clearly be advantageous to suppress these couplings. This can be achieved by replacing the ^{1}H π pulse in the middle of τ_1 with a selective pulse tailored to invert the methyl ^{1}H spins without affecting the methylene ^{1}H spins.

3. Experimental

Data were collected on a Varian ^{UNITY}*INOVA* spectrometer operating at a ^{1}H resonance frequency of 500 MHz. The sample was prepared by dissolving 20 mg ^{15}N-choline chloride (ISOTEC, Miamisburg, Ohio) in 700 µl D_2O. Refocused INEPT experiments were performed using the pulse sequence shown in Fig. 3, which implements the selective ^{15}N–methyl ^{1}H transfer described in the theory section using a 6.695 ms ^{1}H REBURP pulse [12] centered at the methyl ^{1}H frequency. A time τ_{reb} = 6.4 ms, equal to the effective evolution time of the ^{15}N–methyl ^{1}H coupling during the REBURP pulse, was subtracted from the transfer delay as indicated in Fig. 3. For nonselective INEPT experiments, the REBURP was replaced with a nonselective π pulse and τ_{reb} was set to zero.

To allow efficient testing in the absence of hyperpolarization, the sequence includes a ^{15}N purge element before the recycle delay d_1 to ensure that the system reaches a consistent state at the start of each transient. This measure is necessary because it is impractical to allow full relaxation of the choline ^{15}N spin after each transient owing to its very long T_1. The sequence includes a ^{15}N $\pi/2$ pulse immediately prior to acquisition in order to purge any ^{1}H coherence that remains antiphase with respect to ^{15}N after the refocusing period. In the absence of this pulse, intermittent phase aberrations were observed in the methyl ^{1}H resonance.

For ^{15}N T_1 measurements by inversion-recovery, the pulse sequence of Fig. 3 was modified by adding a ^{15}N π pulse and a variable recovery delay immediately before the ^{1}H purge pulse. For these experiments, the ^{15}N purge element before d_1 was removed and d_1 was increased to 600 s.

Data analysis was performed in MATLAB (The MathWorks, Natick, MA) using scripts developed in house. Spectral data were quantified by fitting to a complex Lorentzian lineshape function, except for inversion-recovery data, which was quantified by integration. A downhill simplex algorithm was used for least-squares data fitting, and uncertainties in the extracted parameters were estimated using a bootstrap Monte Carlo method [13].

The value of τ_{reb}, which is subtracted from the INEPT transfer delay in order to account for evolution of the ^{15}N–methyl ^{1}H scalar coupling during the long REBURP pulse, was determined using a numerical simulation of the pulse sequence. Calculations were performed in GAMMA v4.1.2 [14] in Hilbert space using a spin system of practical size, consisting of one ^{15}N and six methyl ^{1}H spins, with J_m = 0.82 Hz. The ^{1}H resonance frequency was set to 500 MHz and the carrier frequencies were set on resonance with the ^{15}N and methyl ^{1}H spins. The REBURP and the nonselective pulses were simulated with finite widths corresponding to the experimental

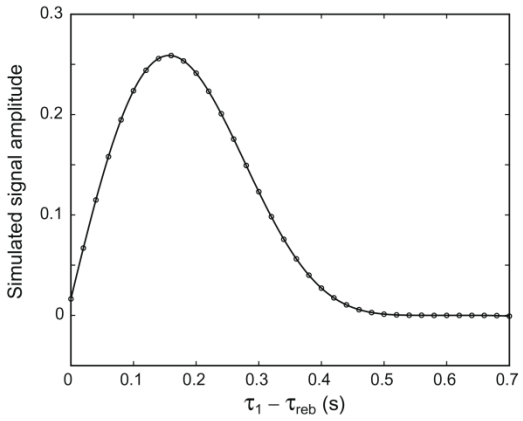

Fig. 4. Numerical simulation of the selective ^{15}N-to-^{1}H INEPT pulse sequence acting on a simplified spin system. Circles are simulated methyl ^{1}H signal amplitudes for different values of the INEPT transfer delay ($\tau_1 - \tau_{reb}$). The line was calculated using a modified form of Eq. (1) with parameter values from a least-squares fit to the data. This fit was used to determine τ_{reb}, the effective evolution time of the ^{15}N–methyl ^{1}H coupling during the sequence's REBURP pulse.

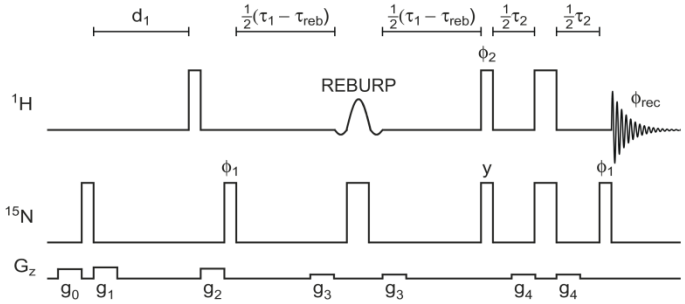

Fig. 3. Selective refocused INEPT pulse sequence for coherent polarization transfer from ^{15}N to methyl ^{1}H in ^{15}N-choline. Narrow (wide) rectangles denote radiofrequency pulses with a tip angle of $\pi/2$ (π), applied with B_1 field strengths of 23.9 kHz for ^{1}H and 15.6 kHz for ^{15}N. The shaped ^{1}H pulse is a 6.695 ms REBURP [12] centered on the methyl ^{1}H frequency. A four step phase cycle ($\phi_1 = x, x, x, x$; $\phi_2 = x, y, x, y$; $\phi_{rec} = x, y, x, y$) was used to suppress signals originating from ^{1}H magnetization and to prevent carry over of signal from one transient to the next. A recycle delay d_1 of 60 s (~0.25 T_1) was used. Since it is impractical to make this delay long enough to allow full relaxation of the choline ^{15}N spin, a purge element consisting of a ^{15}N $\pi/2$ pulse sandwiched by gradients g_0 and g_1 is used to eliminate ^{15}N magnetization at the start of d_1, ensuring a consistent starting magnetization for all experiments. A ^{1}H purge element comprising a ^{1}H $\pi/2$ pulse and gradient g_2 is used at the start of each transient. Gradients g_3 and g_4 are used to suppress coherence transfer pathways created by imperfect π pulses.

values. Relaxation and phase cycling were neglected. The pulse sequence shown in Fig. 3 was simulated, and the methyl ^{1}H signal amplitude was calculated, for each of a series of values of the INEPT transfer delay ($\tau_1 - \tau_{reb}$). The signal data, shown in Fig. 4, was then subjected to least-squares fit to a version of Eq. (1) appropriate for a system containing six methyl ^{1}H spins and including τ_{reb} as an adjustable parameter, resulting in the value of τ_{reb} = 6.4 ms used experimentally.

4. Results and discussion

Fig. 5 shows a spectrum of ^{15}N-choline recorded using the selective ^{15}N-to-^{1}H INEPT sequence of Fig. 3, alongside a ^{15}N-detected spectrum of the same sample recorded in a similar measurement time. It is not meaningful to compare these spectra quantitatively because they were both recorded using a probe that is optimized for direct heteronuclear observation, a factor which diminishes the sensitivity advantage of ^{1}H detection. However, even under these unfavorable circumstances the sensitivity to ^{15}N magnetization is more than an order of magnitude better in the selective INEPT spectrum (Fig. 5a) than in the ^{15}N-detected spectrum (Fig. 5b).

A modified version of the selective ^{15}N-to-^{1}H INEPT experiment was used to measure the ^{15}N longitudinal relaxation time of ^{15}N-choline in D_2O solution, yielding a value of $T_1 = (217 \pm 38)$ s (Fig. 6). This is comparable to the value $T_1 = (285 \pm 12)$ s previously reported by Gabellieri et al. [3] for ^{15}N-choline in 90% H_2O/10% D_2O.

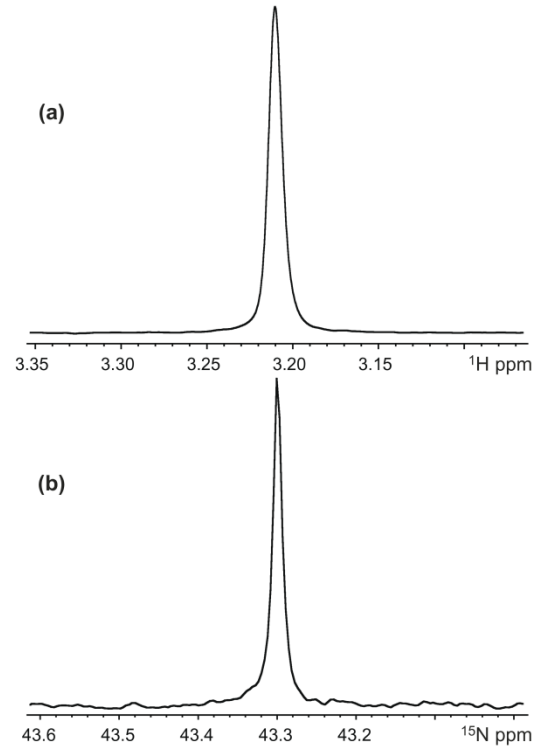

Fig. 5. (a) ^{1}H spectrum of ^{15}N-choline recorded using the selective ^{15}N-to-^{1}H INEPT sequence of Fig. 3. Only the methyl resonance is shown. (b) Single-pulse ^{15}N spectrum of ^{15}N-choline, recorded with tip angle $\pi/2$. Spectra (a) and (b) were each collected on the same Varian AutoX Dual Broadband probe, taking the sum of four transients with a recycle delay of 60 s. Monte Carlo fits of (a) and (b) to Lorentzian lineshapes show that, relative to direct ^{15}N detection, the fractional uncertainty in the initial ^{15}N magnetization is reduced by a factor of 11.0 when using the selective ^{15}N-to-^{1}H INEPT sequence, even though the probe design is optimized for the ^{15}N channel.

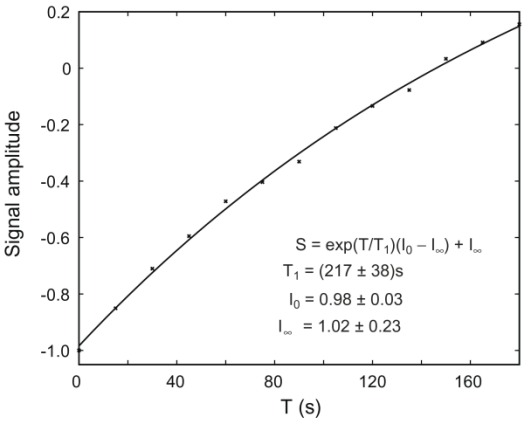

Fig. 6. Measurement of the ^{15}N longitudinal relaxation time of ^{15}N-choline in D_2O solution using a modified version of the pulse sequence shown in Fig. 3. The experiment was repeated for 13 values of the inversion-recovery delay T = 0.001, 15, 30, 45, ..., 180 s. Crosses are experimental methyl ^{1}H signal amplitudes obtained by integrating the spectral data. The line was calculated using the indicated equation and parameter values from a least-squares fit to the data.

A series of ^{15}N-choline ^{15}N-to-^{1}H INEPT spectra were recorded using both selective and nonselective versions of the pulse sequence of Fig. 3 with values of the transfer delay τ_1 ranging from 6.4 ms to 700 ms. The methyl ^{1}H signal amplitudes observed in these experiments are plotted in Fig. 7. The selective INEPT sequence allows ^{15}N-choline to be detected with 52% greater sensitivity than the nonselective sequence, comparing the maximum signal amplitude observed in each case. In the Theory section, the amplitude of the methyl ^{1}H signal was predicted as a function of the transfer delay for the selective (Eq. (1)) and nonselective (Eq. (2)) experiments using a product operator analysis. By fitting the

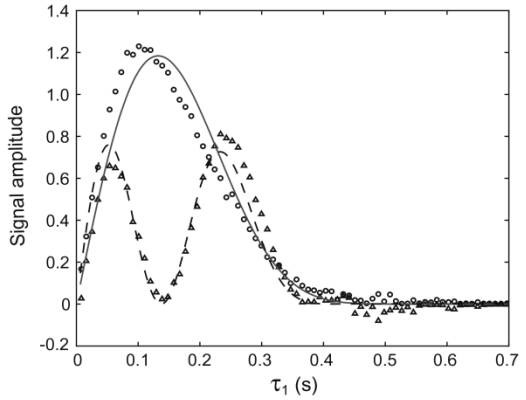

Fig. 7. Amplitude of the methyl ^{1}H signal observed in ^{15}N-to-^{1}H INEPT spectra of ^{15}N-choline using selective (circles) and nonselective (triangles) versions of the pulse sequence shown in Fig. 3, as a function of the INEPT transfer period τ_1. The lines were calculated using Eq. (1) (solid line) and Eq. (2) (dashed line) with parameter values from a least-squares fit to the data.

observed signal amplitudes to Eqs. (1) and (2), the optimal length of τ_1 for each experiment can be determined, as well as precise values of choline's ^{15}N–^{1}H coupling constants.

A simultaneous least-squares fit to both datasets yields parameter values $A_{sel} = 0.632 \pm 0.001$, $A_{non} = 1.000 \pm 0.005$, $J_m = (0.817 \pm 0.001)$ Hz, $J_b = (3.64 \pm 0.01)$ Hz, and $C = 0.000 \pm 0.001$. These values for the coupling constants are similar to ones derived from previously published ^{1}H–^{14}N values ($J_m = 0.80$ Hz and $J_b = 3.61$ Hz) [15] or observed recently [6] with ^{15}N-choline ($J_m = 0.8$ Hz and $J_b = 3.7$ Hz). The value of the smaller ^{15}N–methylene ^{1}H coupling constant was found to have a negligible effect on the fitting process, so this parameter was fixed at a reasonable value of $J_a = -0.57$ Hz.

Note that, for experiments using the selective and nonselective versions of the pulse sequence of Fig. 3 on the same spectrometer hardware and sample, the constants in Eqs. (1) and (2) should ideally be the same. The observation that A_{sel} is smaller than A_{non} may be due to signal losses during the selective sequence's REBURP pulse. Comparing the values of A_{sel} and A_{non} from the least-squares fit it appears that 36% of the signal is lost in this way. This can be attributed in part to miscalibration of the REBURP pulse. A three pulse sequence ($\pi/2 -$ REBURP $- \pi/2$) was used to calibrate the REBURP pulse by seeking pulse width and power parameters that gave the best null signal. It would be more appropriate to choose a calibration sequence that uses the REBURP pulse for inversion, as it is used in the selective INEPT sequence, rather than for refocusing. Another possibility for the relative deviations of the selective and nonselective experiments from the theory is that ^{1}H–^{1}H couplings are neglected in the analytical theory given for the dynamics. Including these numerically is beyond our present computer capabilities.

We have presented a pulse sequence that suppresses the effects of the four methylene protons on the INEPT transfer from ^{15}N to methyl ^{1}H in ^{15}N-choline. Note that the same result can be achieved by selective deuteration of ^{15}N-choline. This approach might provide the additional benefit of increasing the molecule's ^{15}N longitudinal relaxation time and would be an option for DNP experiments. However, the present selective recoupling strategy is clearly advantageous for ^{15}N-choline hyperpolarization using PASADENA. In these experiments, two of the methylene ^{1}H spins derive from a parahydrogen molecule which reacts with an unsaturated precursor to initiate the hyperpolarization process. Although deuteration of the alkene precursor can remove two of the methylene ^{1}H spins, those which supply the spin order cannot be eliminated.

The success of this selective coherence transfer strategy in ^{15}N-choline has clear implications for studies of other hyperpolarized small biomolecules. By directing the spin order to a subset of the possible detection spins, sensitivity is improved. The recoupling strategy demonstrated here accomplishes this by way of a frequency selective π pulse, which simplifies, and often shortens, the polarization transfer step. Similar selective INEPT sequences could be used to improve the sensitivity of the ^{13}C-to-^{1}H polarization transfer experiments demonstrated by Chekmenev et al. in hyperpolarized TFPP [4] by directing the spin order to one of the resolved ^{1}H sites.

The selective ^{15}N-choline transfer presented here also has potentially useful applications to thermally polarized *in vivo* ^{15}N spectroscopy. Pulse sequences can be devised to transfer methyl ^{1}H polarization to ^{15}N for an encoding period and then back to methyl ^{1}H for detection. Such sequences would benefit from choline's long ^{15}N T_1 while making use of the strong thermal polarization of the nine methyl ^{1}H spins. This strategy is equally applicable if the ^{15}N polarization is selectively recoupled to the methylene protons adjacent to the oxygen, which more readily resolve choline from acetylcholine and phospholine [6]. To lengthen the time available for the metabolic interconversion of choline and related compounds, chemical exchange is best encoded in the difference between longitudinal ^{15}N magnetization of the various species, prior to selective polarization transfer.

5. Conclusion

As part of a strategy to improve the sensivity of *in vivo* experiments on hyperpolarized small biomolecules, we have investigated INEPT pulse sequences for the transfer of magnetization from ^{15}N to the methyl ^{1}H spins in ^{15}N-choline. Product operator analysis of a simple refocused INEPT sequence shows that the optimized efficiency of this transfer is diminished by 62% by the action of competing couplings between ^{15}N and choline's methylene ^{1}H spins. A selective INEPT sequence, using a ^{1}H REBURP pulse to suppress undesired couplings during the transfer period, was devised and tested *in vitro* on a thermally polarized ^{15}N-choline sample. It was demonstrated that the selective INEPT sequence leads to a 52% stronger methyl ^{1}H signal than the nonselective version.

Acknowledgments

This work was supported by the Beckman Institute pilot program, "Spin-Polarized Molecules for Structural and Systems Biology". JEO was supported by a Postdoctoral Fellowship from the Natural Sciences and Engineering Research Council of Canada.

References

[1] E.Y. Chekmenev, J. Hovener, V.A. Norton, K. Harris, L.S. Batchelder, P. Bhattacharya, B.D. Ross, D.P. Weitekamp, PASADENA hyperpolarization of succinic acid for MRI and NMR spectroscopy, J. Am. Chem. Soc. 130 (2008) 4212–4213.
[2] K. Golman, R.I. Zandt, M. Lerche, R. Pehrson, J.H. Ardenkjaer-Larsen, Metabolic imaging by hyperpolarized ^{13}C magnetic resonance imaging for in vivo tumor diagnosis, Cancer Res. 66 (2006) 10855–10860.
[3] C. Gabellieri, S. Reynolds, A. Lavie, G.S. Payne, M.O. Leach, T.R. Eykyn, Therapeutic target metabolism observed using hyperpolarized ^{15}N choline, J. Am. Chem. Soc. 130 (2008) 4598–4599.
[4] E.Y. Chekmenev, V.A. Norton, D.P. Weitekamp, P. Bhattacharya, Hyperpolarized ^{1}H NMR employing low γ nucleus for spin polarization storage, J. Am. Chem. Soc. 131 (2009) 3164–3165.
[5] G.A. Morris, R. Freeman, Enhancement of nuclear magnetic resonance signals by polarization transfer, J. Am. Chem. Soc. 101 (1979) 760–762.
[6] R. Sarkar, A. Comment, P.R. Vasos, S. Jannin, R. Gruetter, G. Bodenhausen, H. Hall, D. Kirik, V.P. Denisov, Proton NMR of ^{15}N-choline metabolites enhanced by dynamic nuclear polarization, J. Am. Chem. Soc. 131 (2009) 16014–16015.
[7] J.A. Pfeilsticker, J.E. Ollerenshaw, V.A. Norton, D.P. Weitekamp, Reverse ^{15}N rINEPT with selective recoupling in choline, in: 50th Experimental NMR Conference, Asilomar, 2009.
[8] Y. Boulanger, M. Labelle, A. Khiat, Role of phospholipase A_2 on the variations of the choline signal intensity observed by ^{1}H magnetic resonance spectroscopy in brain diseases, Brain Res. Rev. 33 (2000) 380–389.
[9] R. Katz-Brull, D. Seger, D. Rivenson-Segal, E. Rushkin, H. Degani, Metabolic markers of breast cancer: enhanced choline metabolism and reduced choline–ether–phospholipid synthesis, Cancer Res. 62 (2002) 1966–1970.
[10] E. Sutinen, M. Nurmi, A. Roivainen, M. Varpula, T. Tolvanen, P. Lehikoinen, H. Minn, Kinetics of [^{11}C]choline uptake in prostate cancer: a PET study, Eur. J. Nucl. Med. Mol. Imaging 31 (2004) 317–324.
[11] D.M. Doddrell, D.T. Pegg, W. Brooks, M.R. Bendall, Enhancement of ^{29}Si or ^{119}Sn NMR signals in the compounds $M(CH_3)_nCl_{4-n}$ (M = Si or Sn, $R = 4, 3, 2$) using proton polarization transfer. Dependence of the enhancement on the number of scalar coupled protons, J. Am. Chem. Soc. 103 (1981) 727–728.
[12] H. Geen, R. Freeman, Band-selective radiofrequency pulses, J. Magn. Reson. 93 (1991) 93–141.
[13] W.H. Press, S.A. Teukolsky, W.T. Vetterling, B.P. Flannery, Numerical Recipes in C: The Art of Scientific Computing, second ed., Cambridge University Press, Cambridge, UK, 1992.
[14] S.A. Smith, T.O. Levante, B.H. Meier, R.R. Ernst, Computer simulations in magnetic resonance. An object-oriented programming approach., J Magn. Reson. A106 (1994) 75–105.
[15] V. Govindaraju, K. Young, A.A. Maudsley, Proton NMR chemical shifts and coupling constants for brain metabolites, NMR in Biomedicine 13 (2000).